Nuclear Instruments and Methods in Physics Research A ■ (■■■) ■■■■■

11

13

15

17

19

21

23

25

27

29

31

35

43

Contents lists available at ScienceDirect

Nuclear Instruments and Methods in Physics Research A

journal homepage: www.elsevier.com/locate/nima



The experience of building and operating COMPASS RICH-1

P. Abbon ^m, M. Alexeev ^{a,1}, H. Angerer ^j, G. Baum ^b, R. Birsa ^q, P. Bordalo ^{h,2}, F. Bradamante ^p, A. Bressan ^p, M. Chiosso ⁿ, P. Ciliberti ^p, M. Colantoni ^o, T. Dafni ^m, S. Dalla Torre ^q, E. Delagnes ^m, O. Denisov ^o, H. Deschamps ^m, N. Dibiase ⁿ, V. Duic ^p, W. Eyrich ^e, A. Ferrero ⁿ, M. Finger ^{k,l}, M. Finger Jr^{k,l}, H. Fischer ^f,

C. Franco^h, S. Gerassimov^j, M. Giorgi^p, B. Gobbo^q, R. Hagemann^f, D. von Harrachⁱ, F.H. Heinsius^f, R. Joosten^c, B. Ketzer^j, V.N. Kolosov^{d,3}, K. Königsmann^f, I. Konorov^j, D. Kramer^g, F. Kunne^m, A. Lehmann^e,

S. Levorato ^q, A. Maggiora ^o, A. Magnon ^m, A. Mann ^j, A. Martin ^p, G. Menon ^q, A. Mutter ^f, O. Nähle ^c,

F. Nerling^f, D. Neyret^m, D. Panzieri^a, S. Paul^j, G. Pesaro^p, C. Pizzolotto^e, J. Polak^g, P. Rebourgeard^m, F. Robinet ^m, E. Rocco ⁿ, G. Sbrizzai ^p, P. Schiavon ^p, C. Schill ^f, P. Schoenmeier ^e, W. Schröder ^e,

M. Slunecka k,l, F. Sozzi P, L. Steiger B, M. Sulc M. Svec B, S. Takekawa P, F. Tessarotto H. Teufel B, Teufel B, Teufel B, Tessarotto B, Teufel B

H. Wollny f

^a INFN, Sezione di Torino and University of East Piemonte, Alessandria, Italy

^b University of Bielefeld, Bielefeld, Germany

^c Universität Bonn, Helmholtz-Institut für Strahlen- und Kernphysik, Bonn, Germany

^d CERN, European Organization for Nuclear Research, Geneva, Switzerland

^e Universität Erlangen-Nürnberg, Physikalisches Institut, Erlangen, Germany

f Universität Freiburg, Physikalisches Institut, Freiburg, Germany

^g Technical University of Liberec, Liberec, Czech Republic

h LIP, Lisbon, Portugal

ⁱ Universität Mainz, Institut für Kernphysik, Mainz, Germany

^j Technische Universität München, Physik Department, Garching, Germany

k Charles University, Prague, Czech Republic

¹ JINR, Dubna, Russia

^m CEA Saclay, DSM/DAPNIA, Gif-sur-Yvette, France

ⁿ INFN, Sezione di Torino and University of Torino, Torino, Italy

o INFN, Sezione di Torino, Torino, Italy

P INFN, Sezione di Trieste and University of Trieste, Trieste, Italy

q INFN, Sezione di Trieste, Trieste, Italy

ARTICLE INFO

Keywords: COMPASS RICH MAPMT

Photon detection

63

65

51

ABSTRACT

COMPASS RICH-1 is a large size gaseous Imaging Cherenkov Detector providing hadron identification in the range from 3 to 55 GeV/c, in the wide acceptance spectrometer of the COMPASS Experiment at CERN SPS.

It uses a 3 m long C₄F₁₀ radiator, a 21 m² large VUV mirror surface and two kinds of photon detectors: MAPMTs and MWPCs with CsI photocathodes, covering a total of 5.5 m². It is in operation since 2002 and its performance has increased in time thanks to progressive optimization and mostly to a major upgrade which was implemented in 2006.

The main characteristics of COMPASS RICH-1 components are described and some specific aspects related to the radiator gas system, the mirror alignment, the MWPC electrical stability and the readout electronics are discussed.

Some key features of the event reconstruction and the PID analysis are presented together with results from the COMPASS RICH-1 performance characterization study.

© 2010 Published by Elsevier B.V.

Corresponding author. Tel.: +39 040 3756228; fax: +39 040 3576258. E-mail address: Fulvio.Tessarotto@ts.infn.it (F. Tessarotto).

On leave from JINR, Dubna, Russia.

³ On leave from IHEP, Protvino, Russia.

1. COMPASS RICH-1

The COMPASS Experiment [1] at CERN SPS investigates the nucleon spin structure and the spectroscopy of hadrons; it has a

0168-9002/\$ - see front matter © 2010 Published by Elsevier B.V. doi:10.1016/j.nima.2010.10.102

75

Please cite this article as: P. Abbon, et al., Nucl. Instr. and Meth. A (2010), doi:10.1016/j.nima.2010.10.102

67

69

71

73

² Also at IST, Universidade Técnica de Lisboa, Lisbon, Portugal.

2.5

2.7

29

31

69

71

73

75

77

79

81

83

85

87

89

91

115

133



33 35

37

39

41 43

45 47

49

51 53

55 57

59 61

63

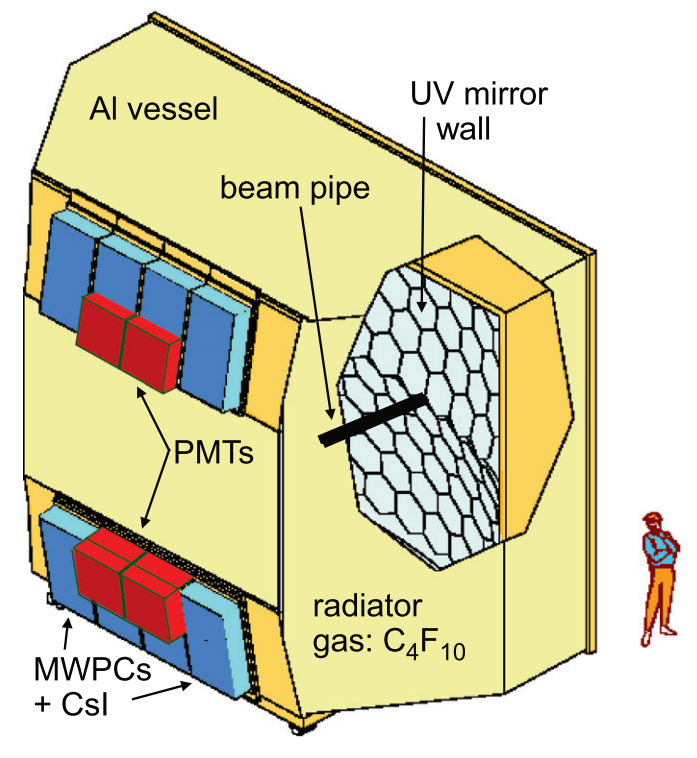


Fig. 1. Artist view of COMPASS RICH-1.

high luminosity fixed-target setup with a two-stage, large angle and large momentum acceptance spectrometer [2].

Hadron identification requirements in COMPASS are quite challenging: good π -K separation from 3 to 55 GeV/c over an angular acceptance of ± 250 mrad in the horizontal plane and \pm 180 mrad in the vertical plane, with beam rates up to 40 MHz and trigger rates up to 20 kHz. Minimum material could be introduced in the region of the spectrometer acceptance (20% X_0) and even less in the beam region (2% X_0).

The COMPASS RICH-1 detector [3,4] (see Fig. 1) provides the required PID performance using a 3 m long gaseous C₄F₁₀ radiator, a 21 m² large focusing VUV reflecting surface and two kinds of photon detectors: MAPMTs and MWPCs with CsI photocathodes, placed outside of the acceptance and covering a total surface of 5.5 m^2 .

It has been designed in 1996 and it is in operation since 2002; its performance has increased in time thanks to progressive optimization and mostly to a major upgrade which was implemented in 2006.

2. The vessel and the C_4F_{10} radiator gas system

Hadron identification in the high momentum domain imposes the use of a gas radiator; the large acceptance of the COMPASS spectrometer and the spectrometer architecture lead to a large volume vessel (about 80 m³).

The tight mechanical tolerances imposed to the production of all elements allowed interfacing the light front and rear vessel walls in the acceptance region, the support frames for the photon detectors and the net-like mechanical structure supporting the mirrors to the aluminium vessel with minimal leaks and mechanical stresses. The beam region is occupied by a light pipe, filled with helium.

The radiator gas, C_4F_{10} , is the heaviest fluorocarbon in gaseous phase at STP and guarantees both low Cherenkov thresholds and low chromatic dispersion; its pressure inside the vessel is kept constant with respect to the atmospheric pressure within 10 Pa by

a dedicated gas system [5] which continuously circulates the gas in a closed loop circuit at a rate of about 2 m³/h. Water vapour and oxygen contaminations are removed by Cu catalyst filters (operated at 40 °C) and 5A molecular sieves (at 15 °C); the resulting levels of contamination are below 1 ppm for H₂O and below 3 ppm for O₂.

Part of the C_4F_{10} is kept in liquid phase inside a storage tank: this buffer allows to compensate for the atmospheric pressure variations and the leaks (which typically are at the level of 80 l/day); before and after the COMPASS running periods all the C₄F₁₀ is recovered in the storage tank, in liquid phase. To avoid the formation of thermal gradients inside the radiator vessel a dedicated system provides a 20 m³/h circulation flow.

Light transmission values larger than 88% in the VUV wavelength domain of the CsI-based photon detectors (165-210 nm), close to the limit provided by Rayleigh scattering process, are routinely obtained. A dedicated cleaning procedure needs to be applied before usage to the commercially available C₄F₁₀, which is full of impurities [6]: the C_4F_{10} circulates in closed loop through activated carbon and 3A molecular sieves and condenses in a cold section where the gas component is vented out, resulting in a typical material loss between 10 and 20%.

The levels of O₂ and H₂O contamination and the total amount of C₄F₁₀ in the system are continuously monitored while the transparency is frequently checked by measuring the light transmission in an automated system based on a UV lamp, a monochromator and PMs; the stability of the radiator gas mixture (typically: $C_4F_{10}/N_2 =$ 97/3) is measured by a sonar-based system.

Regular checks and immediate emergency interventions are granted by experts on call during the entire running period.

3. The mirror system and mirror alignment

The RICH-1 mirror system [7] is a 21 m² VUV reflecting wall divided in two spherical surfaces of 6.6 m radius, focusing the Cherenkov ring images on the photon detectors placed above and below the acceptance region. It is formed by 116 spherical mirror units (68 regular hexagons with 522 mm long diagonal and 48 pentagons), made by an 80 nm thick Al layer deposited on 7 mm thick borosilicate glass substrate and covered by a protective layer (30 nm of MgF_2) .

All mirrors have been characterized before installation: they exhibited good optical quality (radius: 6606 \pm 20 mm, 95% energy spot size: 1.65 ± 0.45 mm, surface roughness r.m.s.: 1.26 ± 0.11 nm) and high VUV reflectance (83-87% in the range 165-200 nm); except a short term degradation at small wavelengths, the reflectance remains stable in time.

To minimize the amount of material in the acceptance the mechanical structure supporting the mirror wall has a net-like configuration, where the nodal points lay on a sphere with a precision of ± 1 mm (a dedicated mould was manufactured for the assembly of the spherical surfaces). The mirrors are arranged in a mosaic-type composition with small clearance between them (4% loss of the total reflecting surface) and suspended to the nodal points via a joint which allows small, controlled angular

After assembling the wall, the mirrors were individually aligned inside the RICH-1 vessel using the theodolite autoreflection method: the theodolite axis is oriented along the straight line joining its centre and the centre of the nominal mirror sphere (reference line); the mirror is then rotated until a laser beam along the reference line is reflected back on the same line. An accuracy of 0.1 mrad is achieved by this procedure.

The mirror alignment status has been checked after each COMPASS run: significant misalignments were only detected at

the end of the first run (up to 1 mrad), while no further displacements larger than 0.2 mrad were detected later.

The alignment check based on the theodolite autoreflection procedure implies risky and difficult operations: opening the RICH-1 vessel, mounting a scaffolding structure inside it and working close to the mirrors. In order to monitor the mirror alignment during the data taking and to avoid repeating the above-mentioned risky operations an original online mirror alignment monitoring method [8] has been developed and implemented in 2007 for COMPASS RICH-1: a rectangular grid is placed inside the vessel close to the front wall and high resolution images of this grid, reflected by the mirrors, are recorded by four cameras fixed on the vessel.

The rectangular grid image is observed by a camera as a set of intersected conics: if neighboring mirrors have a relative misalignment, the conics lines appear to be broken and the shift of the line images provides the direction and the amount of the relative misalignment; the individual calibration constants needed for each mirror position to apply this procedure have been previously measured in a laboratory study.

A similar algorithm is applied to the comparison of images collected at different times, after the subtraction of possible effects due to the movements of the camera (disentangling is easy thanks to optical targets fixed on the mirror support frame): this measurement has confirmed the stability of the mirror orientation during the running period and allowed to detect many slow continuous motions: the maximum observed tilt is $110~\mu rad$.

By the use of photogrammetry for the geometrical description of the grid and for the complete characterization of each camera with its optical system it is possible to extract from the images the absolute position of the centre of curvature of each individual mirror [9].

4. The MWPCs with CsI photocathodes

In its original version RICH-1 [3] used as photon detectors eight MWPCs with 576 \times 1152 mm² active area, equipped with CsI-coated photocathodes. The main parameters of the MWPCs (optimized by the RD26 Collaboration) are: anode–cathode gaps =2 mm, anode wires diameter $=20~\mu\text{m},$ pitch =4 mm, cathode wires diameter $=50~\mu\text{m},$ pitch =2 mm, 8×8 mm² cathode pads (82 944 pads in total). Tight tolerances have been imposed to these parameters (50 μm for the anode–cathode gaps, etc.), and to all aspects of the mechanical construction of the MWPCs and the large quartz windows which separate the radiator gas from the pure methane used in the MWPCs.

The CsI coating of the photocathodes was performed at CERN, and dedicated tools and procedures were developed for their transport and handling to avoid exposure to air (in particular to water vapour) which would result in a degradation of the quantum efficiency: during all processes they were kept in a controlled atmosphere (O_2 level below 50 ppm) and flushed with clean, dry gas.

All MWPCs with CsI photocathodes have been tested in the laboratory to provide gains between 10^5 and 10^6 , but they can be stably operated only at gains not exceeding 5×10^4 in the COMPASS experimental environment: for larger gains they exhibit occasional electrical instabilities with long (~ 1 day) recovery time, clearly related to the combined effect of the level of the applied voltage and the ionizing particle flux, as demonstrated by a series of optimization studies and validation tests performed at the CERN Gamma Irradiation Facility.

The front-end electronics is directly plugged on the external side of the photocathode PCB and performs amplification and shaping of the signal; digitization takes place at the detector and the data are transmitted via optical fibres to the COMPASS DAQ system.

The readout in use before the upgrade could provide a single photoelectron detection efficiency around 70% with an integration time of 0.6 μ s, which was also acting as a detector memory and a 3.5 μ s long baseline restoration time, generating data acquisition dead-time.

With a mean number of 14 detected photons for $\beta=1$ particles, a measured Cherenkov angle resolution of 1.2 mrad for single photons and a PID efficiency larger than 95% over a large fraction of the acceptance COMPASS RICH-1 was providing $2\sigma\pi-K$ separation at 43 GeV/c already before its upgrade.

The presence of a large uncorrelated background was limiting the global resolution on the measured Cherenkov angle, for a particle at saturation, to 0.6 mrad on average and severely lowering the efficiency in the very forward region.

5. The RICH-1 upgrade in 2006

To cope with increased beam intensity and trigger rates and to get rid of the uncorrelated background, RICH-1 has undergone an upgrade in 2006: the central region of the photon detectors (25% of the surface) has been instrumented with a fast detection system [10,4] based on MAPMTs coupled to individual fused silica lens telescopes and read out via sensitive front-end digital electronics and high resolution TDCs. The outer regions have been upgraded by equipping the existing photon detectors with a new readout system [11] based on the APV preamplifier [12] with sampling ADCs providing almost negligible dead-time and good time resolution.

For the upgrade 576 MAPMTs, Hamamatsu 4 R7600-03-M16, 16 channels, with UV extended window, have been used, equipped with custom voltage dividers and individual soft iron boxes (against a \sim 200 Gauss magnetic field). The MAPMTs have been submitted to a complete quality control protocol [13,4] including visual inspection, measurements of dark currents and of gain at five different voltages; a typical gain is about 10^7 (at 900 V), with excellent uniformity; no gain reduction is observed up to single photoelectron rate of 5 MHz per channel.

The light concentration system transmits photons in the range from 200 to 700 nm with wide angular acceptance (100% up to 8.3°, 50% at 9.3°), provides a large image reduction (a factor 7.3 in area) with minimal distortion, and complies with the space limitations at the detector (11.5 cm total length). It consists of individual optical telescopes [14,4] for each MAPMT, made of two fused silica lenses: a plano-convex field lens, placed in the focal plane of the mirrors and a biconvex condenser lens with one aspherical surface, providing the large demagnification with reduced image distortions. The image is projected to the plane of the MAPMT photocathode with a total spot size r.m.s. of 1 mm, to be compared to the 4.5 mm pitch of the MAPMT pixels.

The fused silica lenses are made by grinding and polishing procedure with tight tolerances for surface quality and shape, and are coated with a MgF $_2$ antireflection layer. Each lens and each telescope have been controlled [15,4] employing the Hartmann method [16] by a custom setup and analysis code, providing individual characterization of wavefront distortions with respect to ideal optics: the final image displacement introduced by optics imperfections is below 50 μ m for 70% of the telescopes, and in all cases below 150 μ m. A careful mechanical design of the lens support frames allows to reduce the dead areas below 2% of the surface.

Please cite this article as: P. Abbon, et al., Nucl. Instr. and Meth. A (2010), doi:10.1016/j.nima.2010.10.102

^{a)} 109 at

⁴ Hamamatsu Photonics K.K., 325-6, Sunayama-cho, Hamamatsu City, Shizuoka Pref. 480-8587, Japan.

5

7

9

11

13

15

17

19

21

23

25

2.7

29

31

33

35

37

39

41

43

45

47

49

51

53

55

57

59

61

63

65

6. The readout electronics and the DAQ system

The signals from the MAPMTs are read by a fast digital electronics system [17] based on the eight channels CMAD preamplifier-discriminator, an upgraded version in CMOS technology of the MAD4 [18] chip, developed for COMPASS RICH-1. The CMAD is characterized by small noise level (\sim 1 fC), individual channel thresholds, good time resolution and rate capability: it provides full efficiency up to an input rate of 5 MHz per channel. The design of the front-end boards and the optimization of the thresholds setting allows to suppress the MAPMTs cross talk while keeping at $\sim 95\%$ the single photoelectron detection efficiency.

The good time resolution of the MAPMTs is fully exploited thanks to digital cards, called DREISAM, housing the dead-time free F1 TDC [19], which has a time resolution of \sim 110 ps and can stably operate up to 10 MHz per channel input rate and 100 kHz trigger rate.

All the electronics components of the RICH-1 readout system are mounted directly on the detector, forming a very compact setup. Each PCB is coupled to a copper plate providing both efficient electromagnetic shielding and good cooling power: cold water circulates in underpressure condition in thin copper pipes brazed onto the copper plates [17]. The stability and uniformity of the water cooling system performance is the result of numerous modifications of the distribution system and of the operation and maintenance protocols.

Data from the front-end cards are transferred via optical links to a set of CATCH readout-driver modules which concentrate the data and send them via S-LINK transmitter and optical fibre to the DAQ system.

7. PID performance of COMPASS RICH-1

A dedicated reconstruction and analysis package, called RICHONE, has been developed and optimized to perform hadron identification in COMPASS. For each event the RICH-1 data are decoded, the MAPMT hits are selected on the basis of the time information and the MWPCs hits are selected on the base of the time and amplitude information and clustered; all accepted particles (tracks within the RICH angular acceptance and having a momentum between 1.8 and 180 GeV/c) are then correlated to the RICH reconstructed coordinates.

For each particle a wide fiducial area of the photon detectors is defined, where its Cherenkov photons could have arrived, which can sometimes cover both part of the MAPMT and part of the MWPC or part of the upper and part of the lower photon detector set; for each hit reconstructed coordinate inside the fiducial area an algorithm is used to reconstruct the Cherenkov polar and azimuthal angles (in the particle reference frame), including corrections for the individual mirror parameters and the MAPMT optical system crossed by the photon.

The value of an extended likelihood function is computed for five mass hypotheses (e, μ, π, K, p) and one for the absence of signal hypothesis: the maximum is assumed to correspond to the best hypothesis; the identification purity can be improved by requiring the ratio of best to second best hypothesis likelihood to be larger than a fixed value.

For accurate likelihood evaluation the average refractive index of the radiator gas needs to be know at a few ppm levels for both detector types: it is experimentally determined from the RICH-1 data at fixed time intervals and evolved during the intermediate time periods according to the measured changes in the radiator temperature and pressure.

The RICHONE package performs ring pattern recognition too to allow detailed study of the RICH response; this is essential for the fine tuning and optimization of both the RICH detector and the data analysis.

The number of detected photons per ring as function of the Cherenkov angle for rings fully contained in the MAPMT part of the photon detectors is shown in Fig. 2: for particles with $\beta = 1$ there are on average 56 detected photons.

67

69

71

73

75

77

79

81

83

85

87

89

91

93

95

97

99

101

103

105

107

109

121

123

125

127

129

133

The measured single photon resolution in the central region is 2.0 mrad, and the global resolution on the measured Cherenkov angle [20] is less than 0.3 mrad for particles at saturation, in agreement with the single photon resolution value scaled by the square root of the number of photons: this confirms that the background contribution is minimal, thanks to the time resolution of a few ns.

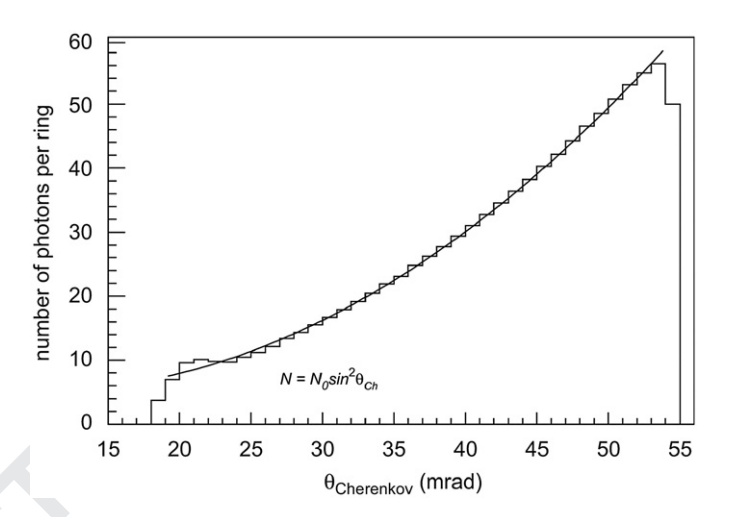


Fig. 2. Number of photons per ring as function of the Cherenkov angle.

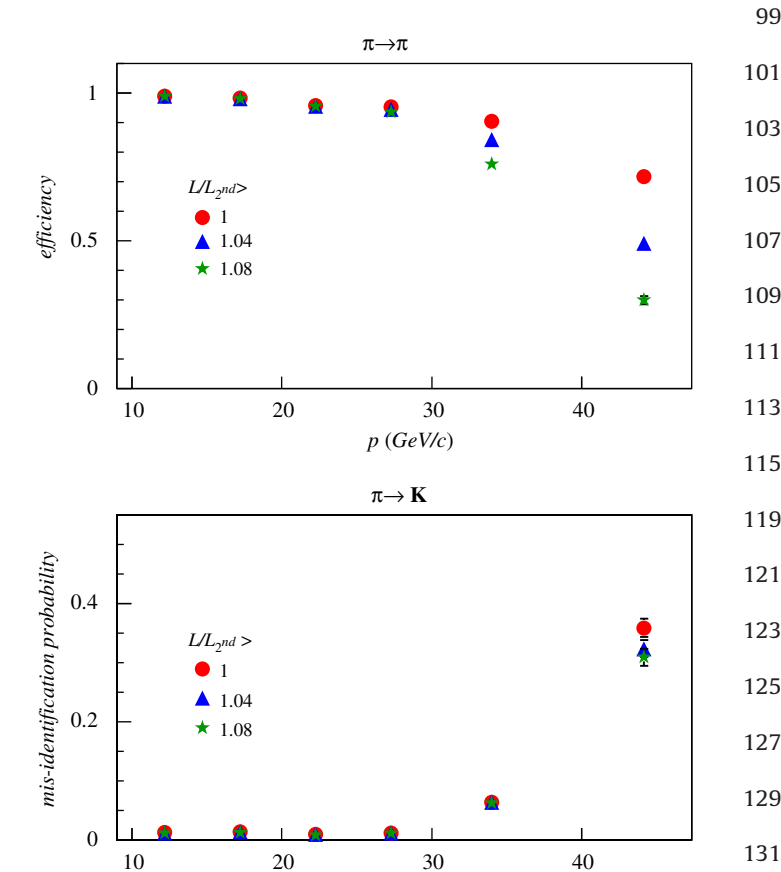


Fig. 3. Efficiency and misidentification probability for π as function of momentum.

p (GeV/c)

Please cite this article as: P. Abbon, et al., Nucl. Instr. and Meth. A (2010), doi:10.1016/j.nima.2010.10.102

69

71

73

75

77

79

81

83

85

87

89

91

93

95

97

123

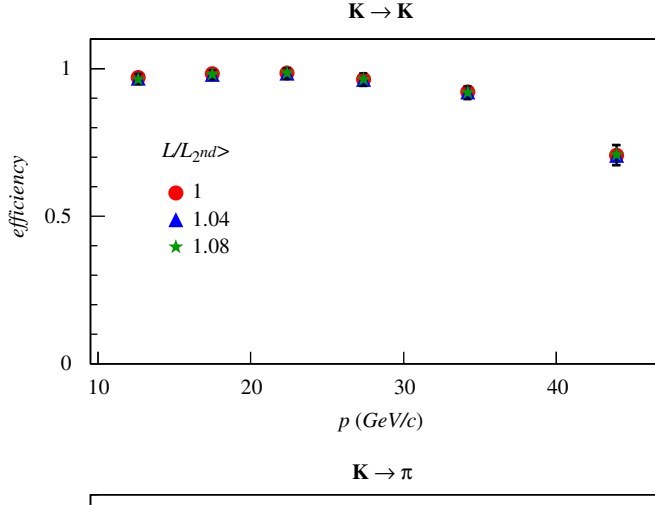
125

127

129

131

P. Abbon et al. / Nuclear Instruments and Methods in Physics Research A ■ (■■■) ■■■-■■■



3

11

13

15

17

19

21

23

25

2.7

29

31

33

35

37

39

41

43

45

47

49

51

53

55

57

59

61

63

65

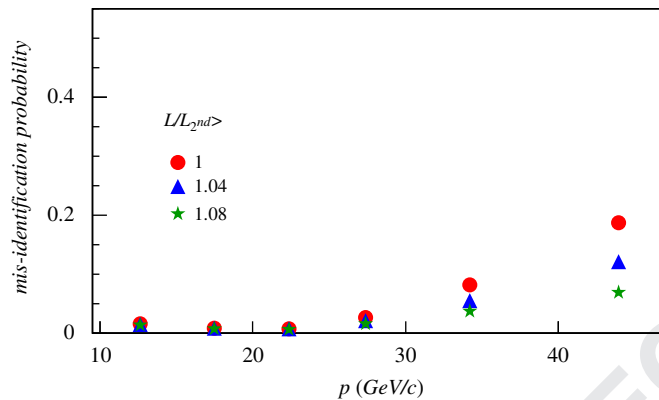


Fig. 4. Efficiency and misidentification probability for *K* as function of momentum.

In the central region, where the ring images produced by high momentum particles are formed, the $2\sigma\pi$ -K separation defined according to the recipe of Ref. [21] is up to 55 GeV/c.

Making use of a sample of kinematically reconstructed K_S^0 $(\phi(1020))$ mesons, the efficiency for π (K) identification has been evaluated as function of particle momenta: Figs. 3 and 4 show the efficiency and the misidentification probability for π (K) for the three most commonly used cuts on the ratio of the best to the second best hypothesis likelihood. For particle momenta below 30 GeV/c the efficiencies are larger than 90% and the misidentification probabilities smaller than 1%; for higher momenta the cut on the likelihood ratio can be tuned to optimize efficiencies or sample purities.

The purity of identified *K* samples depends on the physics channel under consideration: Fig. 5 shows it for standard COMPASS deep inelastic scattering events. In the momentum range below 30 GeV/c the purity is always above 80%, for all cuts on the likelihood ratio.

The identification of hadrons with momenta below the Cherenkov threshold is performed in a very natural way by using the likelihood for the absence of signal hypothesis; thanks to the low background level it turns out to be very effective too: *K* samples with momenta below 9 GeV/c from the decay of $\phi(1020)$ show identification efficiencies larger than 90%.

8. Conclusions

The experience of building and operating COMPASS RICH-1 for almost a decade has been exciting and successful. Original

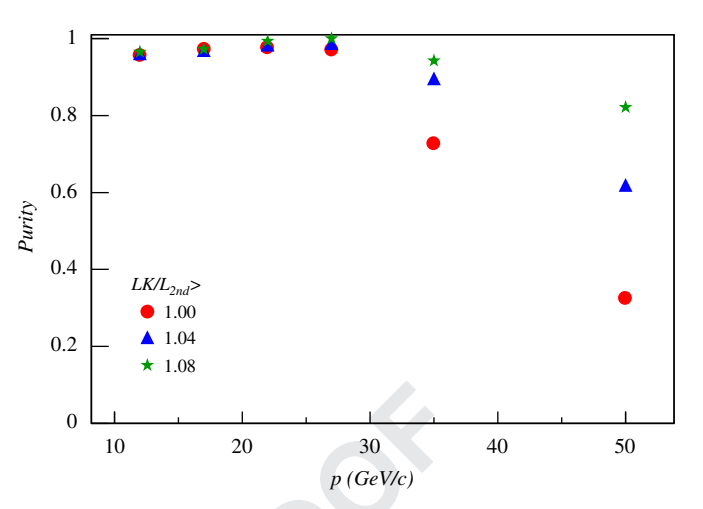


Fig. 5. Purity of *K* samples as function of momentum.

solutions had to be found for several challenging problems in order to reach high and stable PID performance.

As a result of optimizations and of a major upgrade COMPASS RICH-1 offer outstanding hadron identification performance, which have been studied in detail.

Being able to stand beam and trigger rates higher than the present ones, COMPASS RICH-1 is also adequate for the future challenges of the COMPASS Experiment.

References

		٠.
[1]	The COMPASS Collaboration, CERN/SPSLC/96-14,SPSLC/P 297, March 1, 1996; CERN/SPSLC/96-30, SPSLC/P 297, May 20, 1996; Phys. Lett. B 612 (2005) 154; Phys. Rev. Lett. 94 (2005) 202002; Eur. Phys. J. C 41 (2005) 469; Phys. Lett. B 633	99
	(2006) 25; Phys. Lett. B 647 (2007) 8; Phys. Lett. B 647 (2007) 330; Nucl. Phys. B 765 (2007) 31; Eur. Phys. J. C 52 (2007) 255; Phys. Lett. B 660 (2008) 458; Phys. Lett. B 673 (2009) 127; Phys. Lett. B 676 (2009) 31; Phys. Lett. B 680 (2009) 217;	101
	Eur. Phys. J. C 64 (2009) 171; Phys. Rev. Lett. 104 (2010) 241803; Phys. Lett. B 690 (2010) 466; Phys. Lett. B 692 (2010) 240; Phys. Lett. B 693 (2010) 227.	103
	P. Abbon, et al., Nucl. Instr. and Meth. A 577 (2007) 455. E. Albrecht, et al., Nucl. Instr. and Meth. A 502 (2003) 112; E. Albrecht, et al., Nucl. Instr. and Meth. A 518 (2004) 586;	105
[4]	E. Albrecht, et al., Nucl. Instr. and Meth. A 553 (2005) 215. P. Abbon, et al., Nucl. Instr. and Meth. A 616 (2010) 21.	107
[6]	E. Albrecht, et al., Nucl. Instr. and Meth. A 502 (2003) 266. E. Albrecht, et al., Nucl. Instr. and Meth. A 510 (2003) 262.	109
[8]	E. Albrecht, et al., Nucl. Instr. and Meth. A 502 (2003) 236. S. Costa, et al., Nucl. Instr. and Meth. A 553 (2005) 135; M. Alekseev, et al., Nucl. Instr. and Meth. A 595 (2008) 194.	111
	M. Alekseev, et al., Mirror alignment control for Compass RICH-1 detector, these Proceedings. M. Alekseev, et al., Nucl. Instr. and Meth. A 553 (2005) 53;	Q1 13
[]	P. Abbon, et al., Czech. J. Phys. 56 (Suppl. F) (2006) 307; P. Abbon, et al., Nucl. Instr. and Meth. A 567 (2007) 114;	115
	P. Abbon, et al., Nucl. Instr. and Meth. A 572 (2007) 419; P. Abbon, et al., Nucl. Instr. and Meth. A 580 (2007) 906; P. Abbon, et al., Nucl. Instr. and Meth. A 581 (2007) 419.	119
	P. Abbon, et al., Nucl. Instr. and Meth. A 567 (2006) 104. M.J. French, et al., Nucl. Instr. and Meth. A 466 (2001) 359.	121

[13] P. Abbon, et al., Nucl. Instr. and Meth. A 595 (2008) 177.

[14] P. Abbon, et al., Czech. J. Phys. 56 (Suppl. F) (2006) 315.

[15] P. Abbon, et al., Czech. J. Phys. 56 (Suppl. F) (2006) 323.

[17] P. Abbon, et al., Nucl. Instr. and Meth. A 587 (2008) 371;

[18] F. Gonnella, M. Pegoraro, CERN-LHCC-2001-034, p. 204.

[19] H. Fischer, et al., IEEE Trans. Nucl. Sci. NS-49 (2002) 443; H. Fischer, et al., Nucl. Instr. and Meth. A 461 (2001) 507.

[20] P. Abbon, et al., Nucl. Instr. and Meth. A 595 (2008) 233.

P. Abbon, et al., Nucl. Instr. and Meth. A 595 (2008) 204.

[21] T. Ypsilantis, J. Seguinot, Nucl. Instr. and Meth. A 343 (1994) 30.

[16] J. Hartmann, Z. Instrumentenkd 20 (1900) 47;

L.J. Golden, Appl. Opt. 14 (1975) 2391.